



**Oxidative coupling of methane over mixed oxide catalysts  
designed for solid oxide membrane reactors**

Journal:	<i>Catalysis Science &amp; Technology</i>
Manuscript ID	CY-ART-09-2015-001622.R2
Article Type:	Paper
Date Submitted by the Author:	25-Jan-2016
Complete List of Authors:	Farrell, Brittany; University of Michigan, Chemical Engineering Linic, Suljo; University of Michigan, Chemical Engineering



Journal Name

ARTICLE

## Oxidative coupling of methane over mixed oxide catalysts designed for solid oxide membrane reactors

Brittany L. Farrell and Suljo Linic\*

Received 00th January 20xx,  
Accepted 00th January 20xx

DOI: 10.1039/x0xx00000x

[www.rsc.org/](http://www.rsc.org/)

Oxidative coupling of methane is a process that converts methane directly to C<sub>2</sub> products (ethane and ethylene). One of the problems with the technology is that the selectivity and yield to the desired C<sub>2</sub> products is prohibitively low when conventional plug flow reactors are employed. The main reasons for the low C<sub>2</sub> selectivity are the thermodynamic and kinetic preference for undesired products (CO and CO<sub>2</sub>), which are formed through direct methane combustion and sequential ethane and ethylene oxidation. These unselective processes are particularly problematic at high O<sub>2</sub> partial pressures (low CH<sub>4</sub>/O<sub>2</sub> ratios). In order to achieve higher C<sub>2</sub> selectivity, plug flow membrane reactors, utilizing O<sup>2-</sup> conducting oxide membranes, can be utilized. The optimal design of a membrane reactor for OCM would, in addition to the membrane, include a catalyst that is active and selective under the relevant operating conditions, and that can be seamlessly integrated with the membrane. In this contribution we have identified and tested several mixed oxide catalysts which could be integrated into a solid oxide membrane reactor. The tested catalysts included lanthanum gallate doped with strontium and magnesium (La<sub>0.8</sub>Sr<sub>0.2</sub>Ga<sub>0.8</sub>Mg<sub>0.2</sub>O<sub>3-δ</sub>, LSGM), lanthanum manganite doped with strontium (La<sub>0.8</sub>Sr<sub>0.2</sub>MnO<sub>3-δ</sub>, LSM) and lanthanum strontium cobalt ferrite (La<sub>0.8</sub>Sr<sub>0.2</sub>Fe<sub>0.8</sub>Co<sub>0.2</sub>O<sub>3-δ</sub>, LSCF). We show that LSGM and LSGM doped with lithium reached over 90 % selectivity to the C<sub>2+</sub> products at high CH<sub>4</sub>/O<sub>2</sub> operating ratios which are applicable to membrane reactor designs. We have characterized these materials and discussed the strategies for their integration into a membrane reactor system.

### Introduction

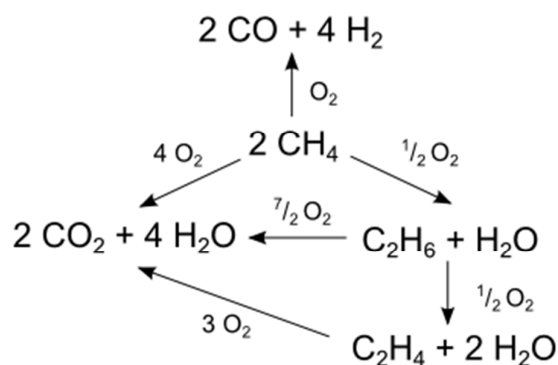
Over the past few decades, methane production has increased due to the availability of shale gas and tight oil.<sup>1,2</sup> Most methane produced is combusted to generate heat and power. A smaller fraction is reformed to produce synthesis gas, a mixture of CO and H<sub>2</sub>, which is used to make chemicals and fuels including methanol, alkanes, and olefins.<sup>2</sup> In these indirect methane conversion processes, the methane reforming and synthesis gas compression account for a large fraction of the overall capital cost (60% or more).<sup>2,3</sup> Therefore, there is significant interest in processes that could convert methane directly into higher value chemicals or fuels without expensive reforming steps.

Methane can be directly converted to ethane and ethylene (C<sub>2</sub>) at low pressure (~ 1 atm) using oxidative coupling. The proposed dominant mechanism of this process on most studied heterogeneous catalysts involves an extraction of a hydrogen atom from methane on a catalyst surface to form a methyl radical (\*CH<sub>3</sub>).<sup>4</sup> The methyl radical is then released from the surface, coupling with another methyl radical in the gas phase to form ethane which can be subsequently

dehydrogenated to form ethylene.<sup>5</sup> Water is formed as a byproduct from the extracted hydrogen and oxygen on the catalyst surface. This process was reported in the early 1980's by Keller and Bahsin and Hinsen and Baerns.<sup>6,7</sup> Since then, there have been a large number of catalysts tested;<sup>8</sup> however, few have shown product yield and conversion that meet broadly accepted techno-economic targets of ~ 35 % yield of C<sub>2</sub> products (ethane and ethylene) per pass with the C<sub>2</sub> selectivity around 90%, at reasonably high rates using undiluted air and methane feeds.<sup>8,9</sup> We note that these techno-economic targets were reported in 1989 for processes converting methane to olefins, and it is possible that slightly different targets would apply today.

The reported C<sub>2</sub> yields in oxidative coupling of methane (OCM) are relatively low because at high operating temperatures (>873 K for most catalysts) required for the activation of strong C-H bonds in methane, CO<sub>2</sub> is the most thermodynamically favorable product.<sup>10</sup> It has been suggested that the undesired CO<sub>2</sub> and CO products (the C<sub>1</sub> products) are formed in two ways: 1) in a parallel reaction path directly from methane and oxygen via combustion and reforming reactions and 2) in sequential reactions, indirectly by further oxidation of ethane and ethylene.<sup>11</sup> The suggested network of reactions involved in oxidative methane coupling is shown in Scheme 1.

Department of Chemical Engineering, University of Michigan, Ann Arbor, MI, USA.  
E-mail: linic@umich.edu



Scheme 1 OCM reaction network

Even a cursory analysis of the network in Scheme 1 sheds light on the difficulties associated with the design of efficient OCM chemical processes. An optimal catalyst needs to extract a hydrogen atom from methane and release the methyl radical. The catalyst needs to accomplish this task without oxidizing ethane and ethylene in sequential reactions. The ease of activation of C-H bonds in ethane and ethylene compared to the C-H bonds in methane represents a significant constraint since the activation of C-H bonds in ethane and ethylene leads to the complete oxidation of these desired product compounds.<sup>12</sup> It can be easily demonstrated that reaction networks where sequential reactions lead to unselective products achieve higher yields to selective products when operated in reactors with low degree of mixing between reactants and products. Therefore, a large fraction of studies performed to date have employed plug flow reactors (PFR) with low mixing. These studies have demonstrated that alkali-promoted oxides and mixed oxides, mainly Li-MgO and NaMnWO<sub>3</sub>, yielded some of the highest measured yields to C<sub>2</sub> products. For example, Li-MgO operated at 973-1073 K reached the C<sub>2</sub> yield of 18-22% with the selectivity to C<sub>2</sub> products of 55-65%,<sup>13</sup> while NaMnWO<sub>3</sub> operated at temperatures higher than 1073 K reached the C<sub>2</sub> yields of 20-30% and the selectivity of 70-80%.<sup>14</sup> Furthermore, a kinetic analysis of the reactions in the network in Scheme 1, performed on an oxide catalyst (La<sub>2</sub>O<sub>3</sub>/CaO was used), illustrated that the reactions leading to C<sub>1</sub> products (CO and CO<sub>2</sub>) exhibited approximately 1<sup>st</sup> order dependence on the partial pressure of O<sub>2</sub>, while the reactions leading to the desired C<sub>2</sub> products showed ½ order dependence on O<sub>2</sub>.<sup>11</sup> This kinetic information suggests that to increase the C<sub>2</sub> selectivity, it is important to operate at relatively low partial pressures of oxygen.

One way to achieve the above discussed optimal operating conditions of *low reactant and product mixing and low partial pressure of oxygen* is to employ membrane plug flow reactors, which allow for a controlled flux of oxygen along the length of the reactor. The main difference between conventional plug flow reactors (PFR) and a membrane plug flow reactor is that in the conventional PFR the local partial pressure of O<sub>2</sub> at the entrance of the reactor is high. This results in high rates of the reactions leading to the combustion products and therefore

low C<sub>2</sub> selectivity. On the other hand, the flux of oxygen species into the membrane PFR is steady along any point in the reactor and the deep oxidation reactions can in principle be better controlled. It is important to note that at high temperatures required for activation of methane C-H bonds, membrane materials that can selectively transport oxygen are mainly limited to solid oxide materials. In this design, oxygen diffuses in the reactor through the solid membrane in the form of an O<sup>2-</sup> ion.<sup>15</sup>

There have been relatively few studies where solid oxide membrane reactors were employed for oxidative coupling of methane.<sup>15-19</sup> While these studies have demonstrated that the selectivity of C<sub>2</sub> products can be increased by using membrane reactors, no system has achieved the above-described techno-economic targets.<sup>17,18,20-22</sup> There are two major factors that have hindered the performance of membrane reactors for OCM. First, in general these systems suffer from low reactant conversion due to the relatively low flux of oxygen through the solid oxide membrane. To increase the oxygen flux, the operating temperature can be increased; however, this has a negative effect on the selectivity to the desired products. Recent advances in solid oxide fuel cell (SOFC) and oxygen separation technologies, including the development of methods to manufacture very thin oxide membranes as well as the discovery of new membrane materials that transport oxygen anions at lower temperatures and that conduct both oxygen ions and electrons, may provide new opportunities for the development of improved oxidative coupling processes.<sup>23,24</sup> Another issue with membrane reactors is that many membranes have been tested without a selective OCM catalyst on the methane side of the membrane, i.e., the membrane served not only to conduct the O<sup>2-</sup> ions but also to catalyze the chemical reactions. Adding a selective catalyst, tailored for OCM, to the membrane surface should increase the C<sub>2</sub> selectivity.<sup>20,25</sup> We note that optimal systems will require catalysts that are not only active and selective for OCM but also that can be seamlessly integrated with the membrane material in a functioning device.

The focus of this contribution is to test the performance of a number of potential OCM catalysts that based on their physical properties can be seamlessly integrated with state of the art solid oxide membranes. This is a necessary starting point for the development of optimal solid oxide membrane-based OCM catalytic systems. The catalysts were selected based on three criteria that make them potentially suitable for the membrane OCM systems. The first criterion was to focus on catalysts that contain elements which have shown high C<sub>2</sub> selectivity in previous OCM studies. In this, we were guided by the work performed by Zavyalova et al. who performed statistical analysis of published data (from over 400 references) reporting the C<sub>2</sub> OCM selectivities and yields of various complex multi-component catalysts. The statistical analysis suggested that in general, catalysts containing La and Mg host oxides exhibit the best performance. It also showed that the addition of a number of dopants including Ba, Sr, Mn, W, Na, Li, or Cs had a positive effect on the C<sub>2</sub> yield for a large fraction of catalysts.<sup>8</sup> Second, catalysts were chosen for their

stability and compatibility with solid oxide membrane materials at fabrication and reaction conditions. Solid oxide membranes are typically fabricated at temperatures above 1273 K to sinter the catalyst layer to the membrane surface, which is required to provide the  $O^{2-}$  ions with a direct pathway between the membrane and catalyst phases. At these processing temperatures, solid state reactions resulting in changes in the composition and properties of the membrane and catalyst materials can occur. Furthermore, it is important to have membrane and catalyst materials with similar coefficients of thermal expansion to avoid stresses on the membrane that can lead to rupture and leakage of reactants. Finally, in addition to the above mentioned requirements of high  $C_{2+}$  selectivity and stability, catalysts that exhibit high  $O^{2-}$  ionic affinity and conductivity at high temperatures were the focus of our attention. This requirement ensures that the transport of  $O^{2-}$  from membrane to the catalyst is facile.

Considering these three criteria, we narrowed our focus to lanthanum gallate oxides doped with strontium and magnesium ( $La_{0.8}Sr_{0.2}Ga_{0.8}Mg_{0.2}O_{3-\delta}$  or LSGM), lanthanum manganite doped with strontium ( $La_{0.8}Sr_{0.2}Mn_{0.98}O_{3-\delta}$  or LSM) and lanthanum ferrite doped with strontium and cobalt ( $La_{0.6}Sr_{0.4}Co_{0.2}Fe_{0.8}O_{3-\delta}$  or LSCF). All three materials contain compositions that the above-mentioned statistical analysis suggested are promising for OCM, they are stable at elevated processing temperatures, and they are able to efficiently shuttle  $O^{2-}$  ions. Our objective was to measure the conversion-selectivity curves of the catalytic materials in OCM under different operating conditions. The measurements were performed in a plug flow packed bed reactor. We found that lanthanum gallate doped with strontium and magnesium ( $La_{0.8}Sr_{0.2}Ga_{0.8}Mg_{0.2}O_{3-\delta}$ , or LSGM) has the highest selectivity to  $C_2$  products at low partial pressures of oxygen. We also found that adding a small amount of lithium in the form of  $Li_2CO_3$  to LSGM slightly improves its overall yield at higher oxygen partial pressures. These results suggest that LSGM is a promising as catalyst for the potential use in a solid oxide membrane reactor.

## Experimental Methods, Results and Discussion

The mixed metal oxide powders used in this study were lanthanum gallate doped with strontium and magnesium ( $La_{0.8}Sr_{0.2}Ga_{0.8}Mg_{0.2}O_{3-\delta}$  or LSGM, Sigma Aldrich), lanthanum strontium manganite ( $La_{0.8}Sr_{0.2}Mn_{0.98}O_{3-\delta}$  or LSM, Praxair) and lanthanum strontium cobalt ferrite ( $La_{0.6}Sr_{0.4}Co_{0.2}Fe_{0.8}O_{3-\delta}$  or LSCF, Sigma Aldrich). Each powder was combined with graphite (300 mesh, Alfa Aesar) in a weight ratio of 1:0.56. The resulting powder was ground by hand using a mortar and pestle then pelletized into cylinders that were 6 mm in diameter and 3.5 mm in length. The carbon was then burned out of the catalyst pellets at 1273 K for 4 hr (ramp rate of 2 K/min) to create porous catalyst pellets weighing 0.11 g each. Lithium was added in the form of  $Li_2CO_3$  (99+%, Acros Organics) to some of the LSGM catalysts in an aqueous solution and dried at 348 K, resulting in catalysts that are 1% Li by weight. Table 1 shows the BET surface area and the median

**Table 1** BET surface area and particle size for the catalysts used in this study

Catalyst	BET Surface Area (m <sup>2</sup> /g)	Particle Size d50 (μm)
LSGM	4	0.8
LSCF	5.5	0.4
LSM	4.77	1.1

particle diameter for the powders used in this study. Due to the fact that these catalysts are designed to be sintered at high temperatures into self-supporting porous structures that can be integrated in membrane reactors, the particle sizes are large and the surface areas are relatively low.

For each experiment, a catalyst pellet was loaded into a ¼" inner diameter alumina tube resulting in a total catalyst weight of 0.11 g. Silica wool was added to both sides of the tube to prevent movement of the catalyst pellet. The alumina tube was placed in a horizontal tube furnace and heated under Ar flow to 1023-1123 K at 2 K/min. After reaching the reaction temperature, the catalysts were held under Ar flow for ~8 hours before air and a certified mixture of 95%  $CH_4$  and 5% He (Cryogenic Gases) were fed using mass flow controllers. The outlet gas was analyzed using a Varian CP 3800 gas chromatography system (GC) equipped with two thermal conductivity detectors and a flame ionization detector. All measured peak areas were compared to gas calibration standards (SCOTTY, Cryogenic Gases) to determine the outlet gas concentrations. Prior to catalyst testing, the system was operated without catalyst to determine the role of gas phase reactions and reactions due to the tube walls and silica wool. At a  $O_2:CH_4:Inert$  molar ratios of 1:3:4 (where the inert gas is a mixture of  $N_2$  from air and He from the methane mixture) and a total flow rate of 100 sccm, the methane conversion without catalyst was 1.3% and 4.1% at 1023 K and 1073 K, respectively. This conversion is approximately 5 % of the conversion obtained using the catalysts at 1023 K, and it does not impact the results reported below.

X-ray diffraction (XRD) was performed using a Rigaku MiniFlex spectrometer. This instrument uses a  $Cu K\alpha$  X-ray source with a graphite monochromator. Data was acquired at a tube voltage and current of 40 kV and 15 mA. XRD patterns were collected with a continuous sweep from  $2\theta$  of 20-80 at a rate of 2  $2\theta$ /min. Phases were identified using the assistance of Jade software.

The data in Figure 1 show the  $C_{2+}$  (ethane, ethylene, propane, and propylene) selectivity and yield as a function of methane conversion and  $CH_4/O_2$  ratio for the tested catalysts. Methane conversion,  $C_{2+}$  selectivity, and  $C_{2+}$  yield were based on molar fractions in the outlet gas and calculated using the following equations:

$$X_{CH_4} = \frac{CO_2 + CO + 2C_2H_6 + 2C_2H_4 + 3C_3H_8 + 3C_3H_6}{CH_4 + CO_2 + CO + 2C_2H_6 + 2C_2H_4 + 3C_3H_8 + 3C_3H_6} \quad (1)$$

$$S_{C_{2+}} = \frac{2C_2H_6 + 2C_2H_4 + 3C_3H_8 + 3C_3H_6}{CO_2 + CO + 2C_2H_6 + 2C_2H_4 + 3C_3H_8 + 3C_3H_6} \quad (2)$$

$$Y_{C_{2+}} = X_{CH_4} * S_{C_{2+}} \quad (3)$$

Solid carbon formed on the catalyst was not included in the carbon balance because there was no visual indication of carbon in the catalyst or in the reactor tubing after the 48 hour tests. XRD measurements supported these visual observations.

The temperature at the inlet of the reactor was 1023 K, and the total inlet flow rate of the air and methane mixture was held constant at 100 sccm. The conditions yielded approximately equivalent space and weight hourly space velocities for all the tested materials. The  $\text{CH}_4/\text{O}_2$  molar ratios at the inlet of the reactor were between 0.8 and 160. The inlet  $\text{CH}_4/\text{O}_2$  ratios are included at the top of each graph for each data point. We note that for the sake of completeness we probed the behavior of the system under some extreme inlet  $\text{CH}_4/\text{O}_2$  molar ratios (i.e., as high as 160). Although the conversions and yields at these conditions are quite low in a packed bed reactor, these ratios were included in our tests since the local partial pressure of oxygen in solid oxide membrane reactors can be very low. We note that in packed bed reactors the  $\text{C}_2$  yield typically reaches a maximum at an inlet  $\text{CH}_4/\text{O}_2$  ratio of  $\sim 3$ .<sup>13</sup> The tested range of molar flow rate ratios allowed for the manipulation of methane conversion up to  $\sim 65\%$  for the given set of operating conditions. We found that over this range of inlet  $\text{CH}_4/\text{O}_2$  molar ratios, oxygen was always the limiting reactant. Oxygen consumption was above 82% in all experiments, and above 90% in most experiments. The catalysts were tested at each reaction condition multiple times over the course of 48 hours. The error bars represent the standard error (the standard deviation of the measurements divided by the square root of the number of measurements) of the measurements at each reaction condition.

The data in Figure 1 show that the LSGM and 1% Li-LSGM catalysts had selectivity to the  $\text{C}_{2+}$  products of  $\sim 90\%$ , achieved at the lowest  $\text{CH}_4$  conversions, which corresponded to the highest inlet  $\text{CH}_4/\text{O}_2$  molar ratios. As the conversion increased (corresponding to a decrease in the inlet  $\text{CH}_4/\text{O}_2$  ratio),

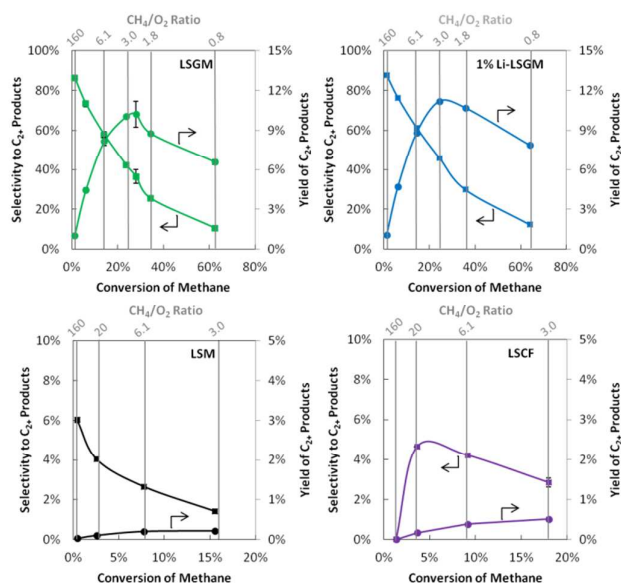


**Figure 1** Selectivity and yield of  $\text{C}_{2+}$  products for each catalyst tested at 1023 K with a total inlet flow rate of 100 sccm. Lines are included to guide the eye.

the selectivity to  $\text{C}_{2+}$  products decreased. The data in Figure 1 show that the yield of  $\text{C}_{2+}$  products for the LSGM catalysts reached a maximum of  $\sim 10\%$  at the  $\text{CH}_4$  conversion of 28% and (inlet  $\text{CH}_4/\text{O}_2$  molar ratio of 3). This yield was slightly increased to over 11% for the LSGM catalysts when 1 wt% Li was added. The selectivity-conversion curves in Figure 1 for LSM show similar trends as those observed for LSGM; however, the  $\text{C}_{2+}$  yields and selectivity were considerably lower. For example, the highest  $\text{C}_{2+}$  selectivity for LSM was  $\sim 6.0\%$  observed at high inlet  $\text{CH}_4/\text{O}_2$  ratio and low  $\text{CH}_4$  conversion. On the other hand, LSCF showed slightly different behavior with very low  $\text{C}_{2+}$  selectivity (approaching zero) at low conversion (high inlet  $\text{CH}_4/\text{O}_2$  ratio). As the conversion increased and the inlet  $\text{CH}_4/\text{O}_2$  ratio decreased, the selectivity to  $\text{C}_{2+}$  products increased to a maximum of  $\sim 4.5\%$  and then decreased at higher conversion.

The data in Figure 2 show the selectivity of each product as a function of the conversion and inlet  $\text{CH}_4/\text{O}_2$  ratio for tested catalysts. This data gives insights into the mechanism of the reaction in the presence of each catalyst. On the LSGM and Li-LSGM catalysts, ethane selectivity was high at low conversion (high inlet  $\text{CH}_4/\text{O}_2$  ratio) and decreased with increasing  $\text{CH}_4$  conversion. The selectivity of ethylene, CO, and the  $\text{C}_3$  products went through a maximum as a function of an increasing  $\text{CH}_4$  conversion. On the other hand,  $\text{CO}_2$  selectivity was low at low conversion (high inlet  $\text{CH}_4/\text{O}_2$  ratio), and increased as the  $\text{CH}_4$  conversion increased. These trends indicate that on LSGM and Li-LSGM, ethane is the primary product, and the main pathway leading to the combustion products includes the sequential oxidation of ethane which can occur through catalytic pathways as well as in the gas phase. The data for the LSM catalyst show that similar to LSGM, the ethane selectivity decreased as the conversion increased. However, unlike LSGM there were also large

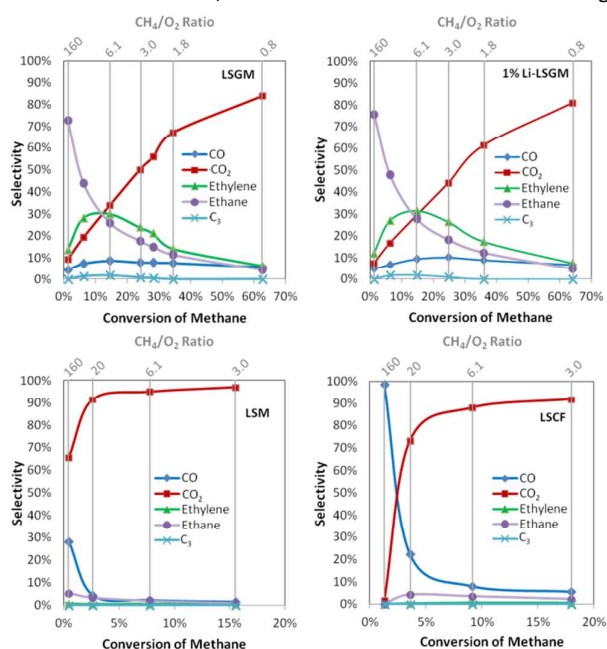


**Figure 2** Selectivity of CO (diamonds),  $\text{CO}_2$  (squares), Ethylene (triangles), Ethane (circles), and  $\text{C}_3$  products (x) as a function of methane conversion and  $\text{CH}_4/\text{O}_2$  ratio for LSGM, 1% Li-LSGM, LSCF, and LSM catalysts. Lines are included to guide the eye.

amounts of the deeper oxidation products (CO and CO<sub>2</sub>) produced at low conversion and high inlet CH<sub>4</sub>/O<sub>2</sub> ratios. This indicates that the deep oxidation reactions, triggered by the activation of C-H bonds in methane, ethane, and ethylene, are more facile on this material compared to LSGM. In contrast, the LSCF catalyst had very high selectivity to CO and no selectivity to ethane at low conversion (high inlet CH<sub>4</sub>/O<sub>2</sub> ratio). This behavior of LSCF suggests that compared to the other tested materials the direct CH<sub>4</sub> partial oxidation to CO and H<sub>2</sub> is a more dominant unselective pathway for this material. In general, we postulate that the low selectivity exhibited by LSCF and LSM is likely due to the presence of transition metals (particularly Co and Fe) in the catalysts. These transition metals are effective catalysts for the deeper oxidation of hydrocarbons.

The catalyst testing demonstrated that the LSGM and Li-LSGM catalysts produced the highest C<sub>2+</sub> yields. To further understand the effect of the reaction conditions on the catalysts, we varied the reactor temperature. The data in Figure 3 a and b show the yield of the combined C<sub>2+</sub> products (ethane, ethylene, propane and propylene) at operating temperatures between 1023 K and 1123 K for the inlet O<sub>2</sub>:CH<sub>4</sub>:Inert (He+N<sub>2</sub>) molar ratio of 1:3:4 with a total flow rate of 100 sccm for the LSGM and Li-promoted LSGM catalysts. These are the conditions that resulted in the highest C<sub>2+</sub> yields. The reported temperatures were measured by a thermocouple in the furnace, and we note that the temperature within the catalyst bed could be higher due to exothermic reactions. While the Li doped catalysts exhibit slightly improved performance, the overall yield of C<sub>2+</sub> products for both catalysts decreases with increased temperature. Furthermore, the ethylene/ethane ratio increased as the operating temperature increased. These results are consistent with the sequential reactions occurring where ethane reacts with oxygen to form ethylene and unselective C<sub>1</sub> products (CO<sub>2</sub> and CO).

For catalysts containing Li, the stability of the catalyst is an important factor because Li can be lost over time when it is converted to LiOH in the presence of oxygen. For instance, many Li-MgO catalysts lose significant activity within the first 20 hours when exposed to OCM reaction conditions.<sup>13</sup> This phenomena, along with the effect on Li-MgO catalyst performance is reviewed in detail in reference 13 and will not be discussed here. Additionally, perovskite materials can have stability issues when exposed to CO<sub>2</sub> and water vapor,<sup>24</sup> which

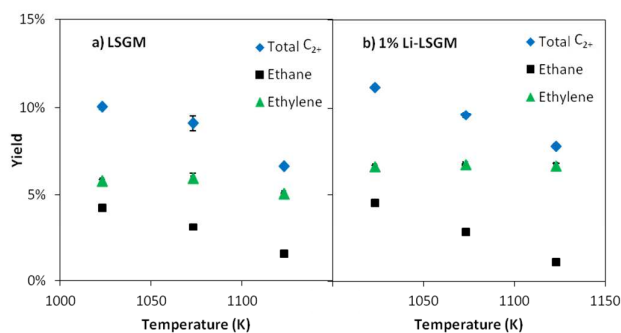


**Figure 3** Effect of temperature on the overall yield of C<sub>2+</sub> products and on the yields of ethane and ethylene for LSGM and 1% Li-LSGM catalyst operating at O<sub>2</sub>:CH<sub>4</sub>:Inert (He+N<sub>2</sub>) ratio of 1:3:4 and total flow rate of 100 sccm: a) LSGM b) 1% Li-LSGM

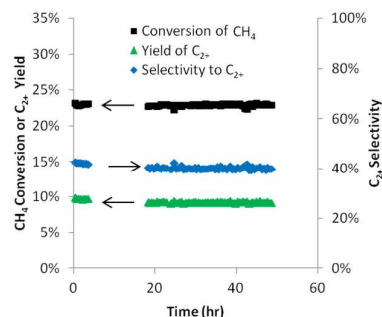


**Figure 4** Stability of 1% Li-LSGM catalyst at 1073 K and O<sub>2</sub>:CH<sub>4</sub>:Inert molar ratio of 1:3:4 at a total of 100 sccm.

are both products in the OCM reaction network. Figure 4 shows data from a stability test of the 1% Li-LSGM catalyst over 48 hours of constant reaction conditions of 1073 K with a O<sub>2</sub>:CH<sub>4</sub>:Inert (He+N<sub>2</sub>) ratio of 1:3:4 and a total flow rate of 100 sccm. The data show that the catalyst was stable over 48 hours under these conditions with little change in conversion of CH<sub>4</sub> or the yield and selectivity of C<sub>2+</sub> products. More testing will need to be completed to determine the long-term stability of the material under reaction conditions.

We have also characterized fresh and used LSGM and 1% Li-LSGM catalysts using XRD. The data in Figure 5 show the normalized X-ray diffraction pattern of fresh LSGM (Fig. 5a), LSGM after heating to 1073 K and cooling back to room temperature in Ar gas (Fig. 5b), and the LSGM catalyst after it has been under reaction conditions at 1073 K for 48 hours (Fig. 5c). Comparison between the diffraction spectra in Figures 5a, 5b, and 5c shows that there are new features that appear in the XRD spectra of the pretreated and used catalysts. We have assigned the new features to SrLaGaO<sub>4</sub> and carbon deposits. There are several peaks that we were unable to assign, including a peak at 2θ of 29.7 that appears in both of the catalysts that have been exposed to methane as well as the

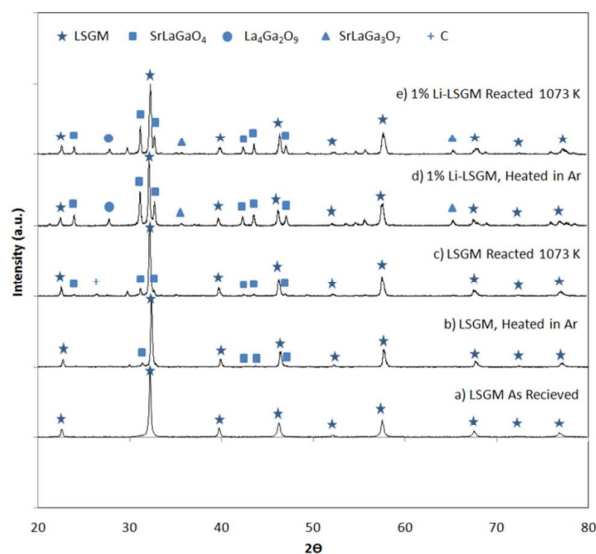


**Figure 5** X-ray diffraction patterns for LSGM catalysts: a) LSGM as received, b) LSGM after heating to 1073 K in Ar c) LSGM after reaction at 1073 K for 48 hours, d) 1% Li-LSGM after heating to 1073 K in Ar, e) 1% Li-LSGM after reaction at 1073 K for 48 hours

LSGM when heated in Ar.  $\text{SrLaGaO}_4$  can be formed when the LSGM is held under reducing conditions at high temperatures.<sup>26</sup> The presence of this impurity phase indicates that the LSGM was partially reduced. The appearance of the new phases after the thermal treatment in an inert environment in Figure 5b suggests that this new phase is not the result of the catalyst operation at the reaction condition, but rather it is a consequence of the thermal reduction of the material. It is important to point out that the conversion and selectivity were stable (at least for 48 hours, the period over which our testing was performed). The data in Figure 5d show X-ray diffraction patterns for the 1% Li-LSGM catalyst after it has been heated in Ar to 1073 K and cooled down to room temperature, while the data in Figure 5e show the diffraction pattern of 1% Li-LSGM after its operation at the reaction conditions at 1073 K for 48 hours. The two catalysts doped with Li show the same  $\text{SrLaGaO}_4$  phase that appeared in the LSGM, along with two new phases that we have assigned as  $\text{La}_4\text{Ga}_2\text{O}_9$  and  $\text{SrLaGa}_3\text{O}_7$ . Comparison of Figure 5d and Figure 5e show that these phases are formed during the thermal reduction of the material (in Argon), and that the materials is otherwise stable at the reaction conditions over 48 hours. Figure 5e also shows that there was no graphitic carbon detected in the used 1% Li-LSGM catalyst. As shown in Figure 4, the selectivity and conversion are steady over this period of time for 1% Li-LSGM.

The data presented above show that LSGM and 1% Li-LSGM are highly selective towards the  $\text{C}_{2+}$  products at high  $\text{CH}_4/\text{O}_2$  ratios and low methane conversion. In addition, this material has several other characteristics that make it potentially useful as a catalyst and/or membrane material in solid oxide membrane OCM reactors. In a solid oxide membrane reactor, the membrane and catalyst materials are layered such that the  $\text{O}^{2-}$  ions are transported through the membrane layer to the methane side catalyst. In an optimal design, the membrane is very thin and dense, and the methane side catalyst is in close contact with the membrane material, enabling it to accept  $\text{O}^{2-}$  ions directly from the membrane. When compared to other  $\text{O}^{2-}$  ion conducting materials, LSGM has relatively high  $\text{O}^{2-}$  ionic conductivity of  $\sim 0.17 \text{ S/cm}$  at 1073 K.<sup>23,27</sup> Therefore, LSGM should be able to accept oxygen anions directly from a membrane and rapidly transfer them to the active centers where the reactions are taking place. Therefore the diffusion of ions through the catalyst in a solid oxide membrane device should not be an issue. The high ionic conductivity of LSGM also suggests that this material could serve a dual role, acting as the catalyst and membrane. Using LSGM as both the membrane and catalyst material has the advantage of avoiding high temperature reactions between dissimilar materials that commonly occur at the temperatures used to create solid oxide membrane devices. Furthermore, in this design thermal stresses that are the consequence of the difference in the thermal expansion coefficients of the catalyst and membrane materials can be minimized. To use LSGM as both a catalyst and membrane material, it will be necessary to provide a way to balance the charge of the system. We note that LSGM transports oxygen in

the form  $\text{O}^{2-}$  ion and to achieve high ion conductivity, which is required to achieve high overall conversion, it is necessary to provide electronic pathways between the oxygen and methane sides of the membrane. This can be done in a few ways: 1) An external electronic connection could be employed to connect the two sides of the membrane, or 2) LSGM can be doped with Mn, Ni, Co, or Fe to induce electronic conductivity into the membrane itself.<sup>28</sup> Both of these methods have advantages and disadvantages. For the external circuit method, an advantage is that the electronic potential difference across the membrane can be controlled, with the option of increasing the oxygen flux electrochemically. A disadvantage is that in order to make a circuit, there must be an electronically conductive material on the methane side which may decrease the selectivity of the overall system. In the case where the membrane itself is electronically conductive, an advantage would be that the system is relatively simple, but the disadvantages are that there is no control over the oxygen flux through the membrane. Furthermore, adding transition metals to LSGM will likely decrease the selectivity of the material to  $\text{C}_{2+}$  products as these metals are very efficient in performing complete and partial oxidation reactions.<sup>29,30</sup>

Another option would be to use LSGM as a catalyst material in conjunction with a different membrane material that exhibits electronic and ionic conductivities. While there are many solid oxide membrane materials that offer mixed ionic and electronic conductivities,<sup>24</sup> the material choice will need to be carefully considered. It is usually required to heat the solid oxide components to temperatures in excess of 1273 K in order to achieve good electronic contact between the membrane and catalyst materials. At these temperatures, it is well known that LSGM can react with the components of many mixed ion-electron conducting oxide materials that could serve as membranes including ceria, zirconia, and LSCF.<sup>31,32</sup> The high temperature solid state reactions result in migration of the metals and new phases between the materials, and the new materials that are formed may or may not have the desired conductive and catalytic properties necessary for a membrane reactor. For example, when lanthanum and zirconium based materials are used in the same device, lanthanum zirconates can be formed.<sup>32</sup> This material can block the transfer of  $\text{O}^{2-}$  across the membrane leading to the loss of methane conversion.

## Conclusions

In conclusion, we have demonstrated that LSGM and 1% Li-LSGM are active and selective as catalysts for oxidative coupling of methane. In packed bed reactor tests, these materials reached over 90 % selectivity to the  $\text{C}_{2+}$  products at high  $\text{CH}_4/\text{O}_2$  operating ratios which are applicable to membrane reactor designs. We have shown that although these materials undergo thermal reduction due to the reducing operating conditions, characterized by high operating temperatures and  $\text{CH}_4/\text{O}_2$  ratios, the new phases that are formed are stable and reactive. Overall, our results indicate

that LSGM and 1% Li-LSGM are promising candidates for catalysts to be used in conjunction with a membrane reactor for oxidative coupling of methane.

### Acknowledgements

We gratefully acknowledge support from United States Department of Energy, Office of Basic Energy Science, Division of Chemical Sciences (FG-02-05ER15686) and National Science Foundation (DMRF- 1436056). B.F. acknowledges that this material is based upon work supported by the National Science Foundation Graduate Research Fellowship under Grant No. DGE 1256260.

### References

- B. P. Statistical, *BP Energy Outlook 2035*, BP, London, UK 2014.
- E. McFarland, *Science*, 2012, **338**, 340–342.
- K. Aasberg-Petersen, C. S. Nielsen, I. Dybkjær and J. Perregaard, *Large Scale Methanol Production from Natural Gas*, Haldor Topsoe.
- J. H. Lunsford, *Catal. Today*, 2000, **63**, 165–174.
- L. Luo, X. Tang, W. Wang, Y. Wang, S. Sun, F. Qi and W. Huang, *Sci. Rep.*, 2013, **3**, 1625.
- G. Keller and M. M. Bhasin, *J. Catal.*, 1982, **73**, 9–19.
- W. Hinsen and M. Baerns, *Chem. Zeitung*, 1983, **107**, 223–226.
- U. Zavyalova, M. Holena, R. Schlögl and M. Baerns, *ChemCatChem*, 2011, **3**, 1935–1947.
- J. C. W. Kuo, C. T. Kresge and R. E. Palermo, *Catal. Today*, 1989, **4**, 463–470.
- Q. Zhu, S. L. Wegener, C. Xie, O. Uche, M. Neurock and T. J. Marks, *Nat. Chem.*, 2013, **5**, 104–109.
- Z. Stansch, L. Mleczko and M. Baerns, *Ind. Eng. Chem. Res.*, 1997, **36**, 2568–2579.
- P. Tang, Q. Zhu, Z. Wu and D. Ma, *Energy Environ. Sci.*, 2014, **7**, 2580–2591.
- S. Arndt, G. Laugel, S. Levchenko, R. Horn, M. Baerns, M. Scheffler, R. Schlögl and R. Schomäcker, *Catal. Rev.*, 2011, **53**, 424–514.
- S. Arndt, T. Otremba, U. Simon, M. Yildiz, H. Schubert and R. Schomäcker, *Appl. Catal. A Gen.*, 2012, **425–426**, 53–61.
- D. Eng and M. Stoukides, *Catal. Rev.*, 1991, **33**, 375–412.
- E. Hazbun, *US Pat.*, 4 791 079, 1986.
- X. Tan, Z. Pang, Z. Gu and S. Liu, *J. Memb. Sci.*, 2007, **302**, 109–114.
- Y. Lu, A. G. Dixon, W. R. Moser, Y. H. Ma and U. Balachandran, *J. Memb. Sci.*, 2000, **170**, 27–34.
- O. Czuprat, T. Schiestel, H. Voss and J. Caro, *Ind. Eng. Chem. Res.*, 2010, **49**, 10230–10236.
- L. Olivier, S. Haag, C. Mirodatos and A. C. van Veen, *Catal. Today*, 2009, **142**, 34–41.
- N. H. Othman, Z. Wu and K. Li, *J. Memb. Sci.*, 2015, **488**, 182–193.
- F. T. Akin and Y. S. Lin, *AIChE J.*, 2002, **48**, 2298–2306.
- T. Ishihara, in *Handbook of Fuel Cells: Volume 4 Fundamentals, Technology, and Applications Part 2*, ed. W. Vielstich, A. Lamm, and H.A. Gasteiger, John Wiley & Sons Ltd, West Sussex, England, Chapter 79, 2003, pp. 1109–1122.
- J. Sunarso, S. Baumann, J. M. Serra, W. a. Meulenbergh, S. Liu, Y. S. Lin and J. C. Diniz da Costa, *J. Memb. Sci.*, 2008, **320**, 13–41.
- N. H. Othman, Z. Wu and K. Li, *J. Memb. Sci.*, 2015, **488**, 182–193.
- E. Djurado and M. Labeau, *J. Eur. Ceram. Soc.*, 1998, **18**, 1397–1404.
- S. P. S. Badwal, S. Giddey, C. Munnings and a. Kulkarni, *J. Aust. Ceram. Soc.*, 2014, **50**, 23–37.
- T. Ishihara, T. Yamada, H. Arikawa, H. Nishiguchi and Y. Takita, *Solid State Ionics*, 2000, **135**, 631–636.
- E. Nikolla, J. Schwank and S. Linic, *Catal. Today*, 2008, **136**, 243–248.
- E. Nikolla, J. Schwank and S. Linic, *J. Catal.*, 2009, **263**, 220–227.
- Z. Bi, Y. Dong, M. Cheng and B. Yi, *J. Power Sources*, 2006, **161**, 34–39.
- J. A. Labrincha, J. R. Frade and F. M. B. Marques, *J. Mater. Sci.*, 1993, **28**, 3809–3815.



In this work, several mixed oxide catalysts for oxidative coupling of methane which could be integrated into a solid oxide membrane reactor are identified and tested.

